PHYSICAL REVIEW D VOLUME 24, NUMBER 4 15 AUGUST 1981

Monte Carlo simulations of systems with fermions

Herbert W. Hamber
Department of Physics, Brookhaven National Laboratory, Upton, New York 11973
(Received 9 April 1981)

We present results of a Monte Carlo evaluation of the path integral for two-dimensional theories with fermions. These include fermions coupled to scalar fields and fermions coupled to Abelian gauge bosons. On a 10 by 10 lattice we have computed expectation values of local operators and correlation functions, from which we have estimated mass gaps. In the case of the coupled gauge-fermion system we find dynamical mass generation for both fermions and gauge bosons. We discuss the phase diagram and the continuum limit of the theory.

I. INTRODUCTION

Recent results have established the usefulness of numerical simulations for the understanding of critical properties in field theories. Until recently this technique had only been applied to systems of bosons. Since fermions are represented in a path integral by anticommuting variables, they are not directly accessible for numerical simulation, but have to be replaced by some appropriate boson functional in the action. Proposals have been made suggesting how to implement this idea[1-3] in practice, and simulations have been performed for small systems with encouraging results. Here we will present results for two models with fermions defined on lattices of 10^2 sites, obtained using an improved version of the boson field method for performing the integrals over the anticommuting fields.

We shall consider theories in which a boson field A_i interacts with a scalar spinless Fermi field[4] on a lattice of N^2 sites. The action is chosen to be of the form

$$S[\bar{\psi},\psi,A]=S_0[A]+\sum_{ij}\bar{\psi}_i M_{ij}(A)\psi_j, \tag{1.1}$$

where $S_0[A]$ is the pure boson action and $M_{ij}(A)$ contains both kinetic and mass terms for the Fermi field, and couplings to the boson field. If the action is not quadratic in the Fermi fields, it can often be reduced to this form by introducing auxiliary boson fields (this is, for example, the case for bilinear interactions). The integration over the Fermi fields is easily performed,

$$\int[d\bar{\psi}][d\psi]e^{-S[\bar{\psi},\psi,A]}=\det[M(A)]e^{-S_0[A]}, \tag{1.2}$$

which leads to an effective action for the A field

$$S_{\rm eff}[A]=S_0[A]-\mathrm{Tr}\ln[M(A)] \tag{1.3}$$

assuming that $\det[M(A)]$ has a definite sign. From this action one can in principle evaluate any correlation function for the A's.

The fermion correlation functions are evaluated by adding sources to the path integral

$$\begin{aligned}Z[\bar{\eta},\eta]&=\int[d\bar{\psi}][d\psi][dA]\exp\left(-S[\bar{\psi},\psi,A]+\sum_{ij}(\bar{\eta}_i\psi_i+\bar{\psi}_i\eta_i)\right)\\&=\int[dA]\exp\left(-S_{\rm eff}[A]+\sum_{ij}\bar{\eta}_i[M^{-1}(A)]_{ij}\eta_j\right)\end{aligned} \tag{1.4}$$

and subsequently taking derivatives

$$\begin{aligned}\langle\bar{\psi}_i\psi_j\rangle&=\frac{\delta^2}{\delta\eta_i\delta\bar{\eta}_j}\ln Z[\bar{\eta},\eta]\Big|_{\bar{\eta}=\eta=0}\\&=\frac{1}{Z}\int[dA]e^{-S_{\rm eff}[A]}[M^{-1}(A)]_{ij},\end{aligned} \tag{1.5}$$

where Z is the normalization integral

$$Z=Z[\eta=\bar{\eta}=0]. \tag{1.6}$$

Many quantities of interest can therefore by evaluated by referring only to $S_{\rm eff}[A]$. Unfortunately, an exact evaluation of $\det[M(A)]$ and $M^{-1}(A)$ for a given configuration $\{A\}$ is much too slow to be useful in a Monte Carlo simulation, and one has to resort to an alternative way of evaluating approximately the fermion determinant (or better, the ratio of two determinants) and the inverse matrix $M^{-1}(A)$.

II. OUTLINE OF THE METHOD

Let us briefly recall the principles of Monte Carlo simulations. In applying the method one constructs by an iterative procedure a sequence of configurations of the fields which eventually

will reach a regime of statistical equilibrium. Starting from a given action $S[A]$ for the field A one is interested in computing averages of the type

$$\langle f(A)\rangle = \frac{1}{Z}\int [dA] f(A) e^{-S[A]} . \tag{2.1}$$

Given an initial configuration $\{A\}$ one generates a new configuration $\{\tilde{A}\}$ by adding to one of the A's at a given site (or link) a random variable with symmetric distribution. In the Metropolis variant of the Monte Carlo method the new configuration is kept if it lowers the action

$$S[A] > S[\tilde{A}] , \tag{2.2}$$

or if the exponential of the difference in actions is less than a random number x with uniform distribution in the interval $[0, 1]$,

$$e^{(S[A]-S[\tilde{A}])} > x . \tag{2.3}$$

Otherwise, the new configuration is rejected and the old one is kept. This procedure guarantees that eventually the probability of encountering any given configuration $\{A\}$ will be proportional to the Boltzmann factor $\exp(-S[A])$ and that averages over configurations converge towards the true averages:

$$\langle f(A)\rangle = \lim_{n\to\infty} \frac{1}{n} \sum_{k=0}^{n} f(A^{(k)}) . \tag{2.4}$$

In order to apply this algorithm to the fermion case we will make use of the identity

$$1 = C\{\det[M(A)]\}^{-1} \int [d\phi] \exp\Big(-\sum_{ij} \phi_i [M^{-2}(A)]_{ij} \phi_j\Big) . \tag{2.5}$$

Here ϕ is a real (one-component) scalar field and C is a numerical constant. After inserting the RHS of this expression in the functional integral and performing the integration over the fermion variables one gets an effective action for the A and ϕ fields,

$$S[A, \phi] = S_0[A] + \sum_{ij} \phi_i [M^{-2}(A)]_{ij} \phi_j . \tag{2.6}$$

If the matrix $M(A)$ is Hermitian one can define $x_i(A) = [M^{-1}(A)]_{ij}\phi_j$ and write

$$S[A, \phi] = S_0[A] + \sum_{i} x_i^{\dagger}(A) x_i(A) . \tag{2.7}$$

We have chosen to compute x by the method of Gaussian iteration. In the process the ith equation in the linear system

$$M_{ij}(A) x_j = \phi_i \tag{2.8}$$

is solved for the variable x_i and its value is determined using the latest set $\{x_j;\ j \neq i\}$ of computed solutions. Then the same process is repeated for the $(i+1)$th equation, etc., until a whole sweep through the index array has been made. This then constitutes one Gaussian iteration. Since $M_{ij}(A)$ is a rather sparse matrix, this procedure is well suited for numerical computation.

If the matrix M is positive definite the process will converge independently of the choice of the initial vector x. On the other hand, a good guess for the initial vector x^0 can significantly speed up the iterative computation of $M^{-1}\phi$. A natural choice is to take for x^0 the vector x that resulted from the application of the Gaussian iteration method *before* the site (or link) variable was changed. Similar considerations apply when computing the fermion propagator by solving iteratively the system of equations

$$M_{ij} U_j = \delta_{i, i_0} .$$

Here again, constantly upgrading U, instead of recomputing it by starting from a trivial configuration (like $U=0$) for every site (or link) variable upgrading, makes a considerable difference in the rate of convergence of the Monte Carlo simulation. From the vector U we immediately obtain the fermion propagator Δ,

$$U_i = \Delta(|i - i_0|, 0) , \tag{2.9}$$

where $|i - i_0|$ is the physical distance on the lattice between the point i and the point i_0.

To further speed up the convergence of the Gaussian iteration, we have found it useful to use relaxation methods, in particular when one approaches a critical point of the fermion theory. In this case the matrix M_{ij} develops a zero eigenvalue (for periodic boundary conditions) due to the presence of a massless fermion.

Almost all the results we will show below were obtained with five to ten Gaussian iterations per site (or link). Although the process of inverting a matrix iteratively for every variable upgrading may appear rather slow in a Monte Carlo simulation, we should point out that with our methods the convergence in quantities like $\langle\bar{\psi}\psi\rangle$ and the fermion propagator turns out to be rather satisfactory, because of the fact that for every upgrading (i.e., for each field configuration) the matrix M^{-1} is evaluated to relatively good accuracy. The error in computing the fermion action with our method is typically of the order of one part in 10^6.

III. A SIMPLE MODEL

Before applying the methods of the preceding section to more complex theories, we have tested them in the context of a simple field theory for

which exact answers can easily be derived. We will consider the model[2] defined by the action

$$S = S_A + S_\psi \tag{3.1}$$

with

$$\begin{aligned} S_A &= \sum_i A_i^2 , \\ S_\psi &= \sum_{ij} \bar{\psi}_i M_{ij} \psi_j , \\ M_{ij} &= -\Delta_{ij} + (m^2 + gA_i^2)\delta_{ij} . \end{aligned} \tag{3.2}$$

Here Δ_{ij} is the lattice version of the Laplacian

$$\Delta_{ij} = \sum_\mu (\delta_{i,i+\mu} + \delta_{i,i-\mu}) - 2D , \tag{3.3}$$

and A_i and ψ_i are a scalar Bose field and a spinless scalar Fermi field,[4,5] respectively. m^2 and g are the two bare parameters of the theory. The fermion propagator in this theory is given by

$$\Delta(i-j) = \langle \psi_i \psi_j \rangle = \left(-\Delta + m^2 + \frac{g}{2} \right)^{-1}_{ij} . \tag{3.4}$$

Table I shows the results obtained from the Monte Carlo simulation on a 10×10 lattice with periodic boundary conditions at $g = m = 1$. The last column with the Monte Carlo data corresponds to 300 sweeps through the lattice, of which the first 100 were discarded. For each upgrading five Gaussian iterations were used.

In this theory the fermion propagator falls off at large distances like

$$\Delta(i-j) \underset{|i-j| \to \infty}{\sim} e^{-\mu |i-j|} ,$$

where μ is the renormalized fermion mass,

$$\mu = (m^2 + g/2)^{1/2} .$$

It is of interest to be able to extract the mass gap from the knowledge of some values for the correlation function. This can be done by taking the Fourier transform of this function on a lattice with finite spatial extension. In this way finite-size effects can be significantly reduced. In other words, the correlation function computed by Monte Carlo simulation on an $N \times N$ lattice of spacing a is fitted (at large distances) to a form

$$Z[-\Delta + \mu_{\mathrm{FT}}^2]^{-1}_{ij} \quad (N \times N) ,$$

where Z is a renormalization constant. μ_{FT} is then the renormalized mass. This method is bound to give the exact answer for a free field theory and can be shown to be effective also for less trivial theories.

It is useful to compute the quantity $\langle \bar{\psi}\psi \rangle = \Delta(0)$ since it has the property of diverging at the critical point $\mu = 0$. To see this we compute in the continuum limit

$$\begin{aligned} \langle \bar{\psi}\psi \rangle &= -\frac{\partial}{\partial m^2} \ln Z \\ &\underset{\mu \to 0}{\sim} -\frac{\partial}{\partial m^2} \int \frac{d^D K}{(2\pi)^D} \ln(k^2 + m^2) , \end{aligned} \tag{3.5}$$

and in two dimensions we get

$$\frac{1}{2\pi} |\ln \mu| . \tag{3.6}$$

In Fig. 1 we have shown the results for $[\Delta(i)]^{-1}$

TABLE I. Monte Carlo results for the fermion correlation function compared to the exact answer for $m = g = 1$ [which corresponds to a mass $\mu = (\frac{3}{2})^{1/2} = 1.2247$].

	3 iter.	30 iter.	300 iter.	Exact
$\Delta(0)$	0.203	0.218	0.217	0.217 54
$\Delta(1)$	0.047 2	0.050 5	0.049 4	0.049 14
$\Delta(2)$	0.011 1	0.012 5	0.012 0	0.011 96
$\Delta(3)$	0.002 7	0.003 2	0.003 1	0.003 11
$\Delta(4)$	0.000 74	0.000 95	0.000 88	0.000 899
$\Delta(5)$	0.000 37	0.000 49	0.000 45	0.000 464
$\ln\Delta(3)/\Delta(4)$	1.29	1.21	1.26	1.24

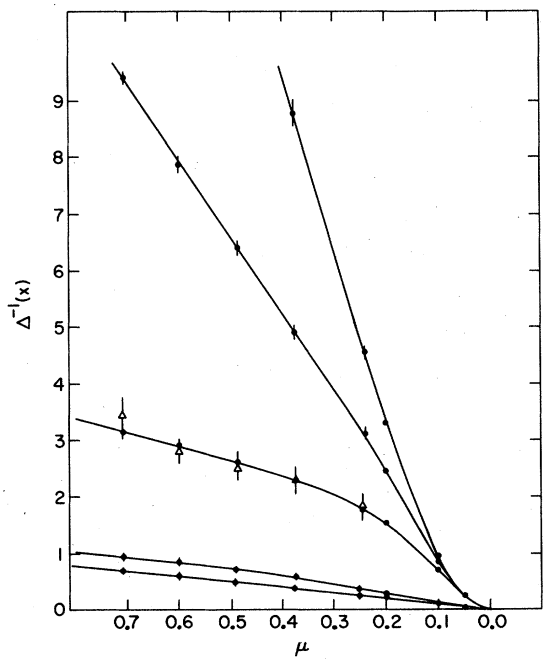

FIG. 1. From above, $\Delta^{-1}(2)$, $\Delta^{-1}(1)$, and $\Delta^{-1}(0)$ as functions of $\mu = (m^2 + g/2)^{1/2}$, the renormalized mass. The two curves at the bottom are $\ln[\Delta(2)/\Delta(1)]$ and μ as determined from the Monte Carlo simulation. The average $\langle A^2 \rangle$ is represented by Δ. The points without error bars are exact results.

$(i=0,1,2)$ and $\ln[\Delta(1)/\Delta(2)]$ as a function of the bare parameter $\mu=(m^2+g/2)^{1/2}$. From the graph we estimate $\mu_c=0.0\pm0.05$ in good agreement with the exact answer $\mu_c=0$. In this case for each value of m and g ($m=g$ here) we used 30 Monte Carlo iterations with five Gaussian iterations per upgrading.

IV. COMPACT QED IN TWO DIMENSIONS

We are now ready to turn to a less trivial example, an Abelian U(1) gauge boson coupled to a spinless scalar fermion. The action is

$$S=S_\theta+S_\psi \tag{4.1}$$

with

$$S_\theta=2\beta\sum_{\text{squares}}(1-\cos\theta_{\mu\nu}) \tag{4.2}$$

and

$$S_\psi=-K\sum_{n,\mu}(\bar\psi_n e^{i\theta_{n\mu}}\psi_{n+\mu}+\bar\psi_{n+\mu}e^{-i\theta_{n\mu}}\psi_n)+\sum_n\bar\psi_n\psi_n\,. \tag{4.3}$$

Here $\theta_{n\mu}$ is a variable that ranges from 0 to 2π and is defined on the oriented links of a square lattice of spacing a, and $\theta_{\mu\nu}$ is the usual lattice curl,

$$\theta_{\mu\nu}=\Delta_\mu\theta_\nu-\Delta_\nu\theta_\mu\,. \tag{4.4}$$

The parameter k is a function of the bare fermion mass m:

$$k=\frac{1}{4+m^2} \tag{4.5}$$

so that $m=0$ corresponds to $k=\frac{1}{4}$. It is instructive to derive the weak-coupling limit of this theory. We set $\beta=\frac{1}{4}g^2$, $\theta_{n\mu}=gA_{n\mu}$, and expand

$$e^{i\theta_{n\mu}}=1+igA_{n\mu}-\tfrac{1}{2}g^2A_{n\mu}{}^2+\cdots\,. \tag{4.6}$$

Substituting this in the action (4.1) and expanding out we get

$$S=\tfrac{1}{4}\sum_{n\mu\nu}(F_{\mu\nu})^2-k\sum_{n\mu}(\bar\psi_n\psi_{n+\mu}+\bar\psi_{n+\mu}\psi_n)-\mu^2\sum_{n\mu}[\bar\psi_n(igA_{n\mu}-\tfrac{1}{2}g^2A_{n\mu}{}^2)\psi_{n+\mu}+\bar\psi_{n+\mu}(-iA_{n\mu}-\tfrac{1}{2}g^2A_{n\mu}{}^2)\psi_n]+\sum_n\bar\psi_n\psi_n\,. \tag{4.7}$$

The field A_μ is now allowed to vary from $-\infty$ to $+\infty$. A weak coupling perturbative expansion could now be developed using the fermion and boson per propagators

$$\Delta(k)=\frac{1}{1-2k\sum_\mu\cos k_\mu}\,,\qquad G_{\mu\nu}(k)=\frac{\delta_{\mu\nu}}{4\sum_\mu\sin^2(\frac{1}{2}k_\mu)}\,, \tag{4.8}$$

and the three- and four-point vertices

$$\Gamma^{(3)}_\mu(\kappa)=2\sin k_\mu\,,\qquad \Gamma^{(4)}_\mu(k)=2\cos k_\mu\,, \tag{4.9}$$

in the momentum-space representation. If we go one step further and take the lattice spacing a to zero after making the replacement

$$\psi_{i+\mu}\to\psi_{(i)}+a\partial_\mu\psi_{(i)}\,,\qquad A_\mu\to aA_\mu\,,\qquad a^2\sum_i\to\int d^2x\,, \tag{4.10}$$

we find the continuum action

$$S_c=\int d^2x\left[\tfrac{1}{4}F_{\mu\nu}{}^2+(\partial_\mu+ieA_\mu)\bar\psi(\partial_\mu-ieA_\mu)\psi+\left(\frac{m}{a}\right)^2\bar\psi\psi\right] \tag{4.11}$$

with β and e related through $\beta=1/(4e^2a^2)$. The generating function for this theory is identical to the one for the massive Schwinger model[6] (i.e., with Dirac fermions), with two fermion flavors, if we neglect spin forces. This can be readily seen by doing the functional integrations over ψ and $\bar\psi$ and using the identity

$$\det[-(\partial_\mu+ieA_\mu)^2+\tfrac{1}{2}\sigma_{\mu\nu}F_{\mu\nu}+m^2]=[\det(\not\partial+ie\not A+m)]^2. \tag{4.12}$$

When the determinant on the right-hand side is replaced by its integral representation

$$(\det M_{\alpha\beta})^n=\int[d^n\bar\psi_\alpha][d^n\psi_\beta]\exp\left(-\int d^2x\bar\psi_\alpha M_{\alpha\beta}\psi_\beta\right), \tag{4.13}$$

two components ($n=2$) are required, which gives the stated result.

In two limits the lattice theory can be exactly solved. One is when $m\to0$ and $g\to0$ (massless fermions in the continuum theory). The other case is when $m\to\infty$, which corresponds to the pure gauge theory.

In the massless limit we start from the continuum theory and use the boson representation[7] to derive the spectrum. In the massless two-component Schwinger model

$$L = i\bar{\psi}(\not{\partial} - ie\not{A})\psi + \tfrac{1}{4}(F_{\mu\nu})^2 , \tag{4.14}$$

with ψ_α^a a two-component Dirac spinor, we make the replacement

$$\psi_{1,2}^a(x) = \left(\frac{\Lambda}{2\pi\gamma}\right)^{1/2} \times \exp\left\{-i\sqrt{\pi}\int_{-\infty}^{x^1} dz[\pi(x^0, z) \pm \partial_1\phi(x^0, z)]\right\}, \tag{4.15}$$

with Λ a cutoff parameter, γ Euler's constant, and $\phi(x)$ a boson field with canonical momentum $\pi(x)$. The boson action density then becomes

$$L_B = \tfrac{1}{2}[(\partial_\mu\phi_a)^2 + (\partial_\mu\phi_b)^2] - \frac{m\Lambda}{\pi\gamma}[\cos\sqrt{\pi}\phi_a + \cos\sqrt{\pi}\phi_b] - \frac{e^2}{2\pi}(\phi_a + \phi_b)^2 . \tag{4.16}$$

After the change of variable

$$\psi_1 = (\phi_a + \phi_b)/\sqrt{2}, \qquad \psi_2 = (\phi_a - \phi_b)/\sqrt{2}, \tag{4.17}$$

we get

$$L_B = \tfrac{1}{2}[(\partial_\mu\psi_1)^2 + (\partial_\mu\psi_2)^2] - \frac{2m\Lambda}{\pi\gamma}\cos\sqrt{2\pi}\psi_1\cos\sqrt{2\pi}\psi_2 - \frac{1}{2}\left(\frac{2e}{\pi}\right)^2\psi_1^2 . \tag{4.18}$$

This shows that for $m = 0$ there is a massive particle of mass $(M/a)^2 = 2e^2/\pi$. (We use the symbol M for dimensionless mass.)

When $k \to 0$ ($m \to \infty$) the fermions become infinitely massive and the model reduces to a pure U(1) gauge theory, which can be solved by transfer matrix techniques. The free energy can be shown to be

$$F = \ln I_0(2\beta) - 2\beta \tag{4.19}$$

and the average plaquette, proportional to the energy density, is given by

$$\langle 1 - \cos\theta_{\mu\nu}\rangle = \tfrac{1}{2}E = -\frac{1}{2}\frac{\partial}{\partial\beta}F . \tag{4.20}$$

From these equations one can derive weak- and strong-coupling expansions which are useful in comparing with the Monte Carlo data:

$$\langle 1 - \cos\theta_{\mu\nu}\rangle = 1 - \beta + \tfrac{1}{2}\beta^3 - \tfrac{1}{3}\beta^5 + \tfrac{11}{48}\beta^7 + \cdots \quad (\beta \ll 1)$$
$$= \frac{1}{4\beta} + \frac{1}{32}\left(\frac{1}{\beta}\right)^2 + \frac{1}{64}\left(\frac{1}{\beta}\right)^3 + \cdots \quad (\beta \gg 1). \tag{4.21}$$

In this always-confining theory a square Wilson loop of area A is given by

$$W(\Gamma) = [I_1(2\beta)/I_0(2\beta)]^A \tag{4.22}$$

and the string tension is therefore

$$T = \ln[I_0(2\beta)/I_1(2\beta)] = \ln\beta + O(\beta^2) \quad (\beta \ll 1) = \frac{1}{4\beta} + O\left(\frac{1}{\beta^2}\right) \quad (\beta \gg 1) . \tag{4.23}$$

In this model the dimensionless gauge boson mass M is equal to the dimensionless string tension.

When the fermions are coupled to the photon the theory is no longer soluble. The fermions give rise to screening and the Wilson loop contains a perimeter contribution. For small β and k we have

$$W(\Gamma) \underset{\substack{\beta\to 0\\ k\to 0}}{\sim} \beta^A + k^P + \cdots . \tag{4.24}$$

Depending on whether $\beta/k \gtrless 1$ the area (or the perimeter) behavior will be more pronounced for small loops (with sides of the order of a few lattice spacings).

Another quantity of interest is the photon propagator defined as a loop of side L and height one. With this definition it is a gauge-invariant quantity and reduces to the usual propagator for weak coupling when the gauge $\theta_\mu = 0$ is chosen for the links in the direction of L. The photon mass determines the exponential falloff of the propagator at large separations

$$G(L) = \left\langle \prod_{\text{square}} e^{i\theta_\mu} + \text{H.c.}\right\rangle \underset{L\to\infty}{\sim} ce^{-ML} . \tag{4.25}$$

The fermion propagator, too, is not a gauge-invariant quantity, but the average

$$\Delta(i-j) = \left\langle \bar{\psi}_i \exp\left(i\sum_{n=i}^{j}\theta_{\mu n}\right)\psi_j\right\rangle, \tag{4.26}$$

is gauge invariant and can be used to define a renormalized fermion mass $m_R = m + \delta m$ such that

$$\Delta(L) \underset{L\to\infty}{\sim} c' \exp\left[-\left(\frac{m+\delta m}{a}\right)L\right]. \tag{4.27}$$

The operator in (4.26) represents two fermions connected by a gauge-field flux tube. In the limit $\beta \to \infty$ the gauge field is frozen (its dynamics is limited to small oscillations around $\theta_\mu = 0$) and in this limit $\delta m = 0$. At $\beta = 0$ the gauge field is entirely random, and we expect in this case that mass renormalization effects will be most significant.

Another gauge-invariant quantity is the expectation value

$$\Delta(0) = \langle \bar{\psi}\psi \rangle , \tag{4.28}$$

which has the property of vanishing as $k \to 0$ and diverging (in two dimensions) when the renormalized mass of the fermions approaches zero. If we call k_c the value of k at which m_R is zero, then for k close to k_c we expect a behavior

$$\langle \bar{\psi}\psi \rangle \underset{k \to k_c}{\sim} A(k_c - k)^{-\theta} \tag{4.29}$$

with θ a critical exponent. $\langle \bar{\psi}\psi \rangle$ represents a fermion bound state (or condenstate) wave function.

The quantities m_R and $\langle \bar{\psi}\psi \rangle$ will turn out to be useful in constructing the phase diagram of the theory. They play here a role similar to the inverse correlation length and the order parameter in spin systems.

We now turn to a discussion of our Monte Carlo results. The numbers shown in the figures and in Tables II–IV were obtained by doing 100 passes on a 10×10 lattice with periodic boundary conditions. During the first 50 passes the system was allowed to reach thermal equilibrium. Then data were collected at every pass. For most of the points more than one run was made in order to put bounds on the statistical and systematic errors. Both ordered and random starts were used for $\beta > 1$. Extensive runs on a 4×4 lattice were also made so that the results could be compared and the extent of finite-size effects determined. These were found sufficiently small for the 10×10 lattice. Thermal cycles with rather different random number generators gave the same answers to within the accuracy of our method (limited by the time of the runs). Typically in a thermal cycle we started from a completely ordered ($\beta = \infty$) or disordered ($\beta = 0$) configuration and changed β by 0.25 after 100 iterations. For selected points 300 iterations and runs on a 20×20 lattice were done. No gauge fixing was used for the gauge field.

Figure 2 shows the behavior of the average plaquette (which is twice the energy density per link for the pure gauge theory) as a function of β for different values of the bare fermion mass. We have noticed that this quantity is barely affected by the presence of the fermions, even at $m = 0$ ($k = \frac{1}{4}$). The continuous line represents the exact answer in the limit of infinite fermion mass ($k = 0$).

TABLE II. Monte Carlo results for $m = 0$. Inverse gauge coupling in column 1, average plaquette in column 2, fermion propagator at the origin (or $\langle \bar{\psi}\psi \rangle$) in column 3, dynamically generated fermion mass δm in column 4, and gauge-boson mass M in column 5.

β	$\langle 1 - \cos\theta_{\mu\nu} \rangle$	$\Delta(0)$	δm	M
0.00	1.00	0.374	1.10	∞
0.25	0.75	0.389	1.05	1.45
0.50	0.59	0.401	0.96	0.85
0.75	0.41	0.420	0.86	0.72
1.00	0.31	0.435	0.75	0.51
1.25	0.22	0.456	0.68	0.33
1.50	0.18	0.467	0.58	0.30
1.75	0.17	0.472	0.57	0.28
2.00	0.14	0.481	0.56	0.25
2.25	0.12	0.487	0.52	0.23
2.50	0.10	0.499	0.48	0.23
∞	0.00	∞	0	0

TABLE III. Monte Carlo results for $m = 0.5$. Inverse gauge coupling in column 1, average plaquette in column 2, fermion propagator at the origin (or $\langle \bar{\psi}\psi \rangle$) in column 3, dynamically generated fermion mass δm in column 4, and gauge-boson mass M in column 5.

β	$\langle 1 - \cos\theta_{\mu\nu} \rangle$	$\Delta(0)$	δm	M
0.00	1.00	0.327	0.70	∞
0.25	0.75	0.333	0.68	1.70
0.50	0.58	0.340	0.56	0.90
0.75	0.36	0.348	0.50	0.57
1.00	0.28	0.354	0.40	0.36
1.25	0.22	0.357	0.39	0.35
1.50	0.17	0.362	0.25	0.30
1.75	0.15	0.363	0.25	0.28
2.00	0.13	0.364	0.25	0.26
2.25	0.11	0.365	0.28	0.25
2.50	0.10	0.367	0.26	0.22
5.00	0.05	0.372	0.12	0.13
∞	0.00	0.379	0.00	0.00

TABLE IV. Monte Carlo results for $m = 1.0$. Inverse gauge coupling in column 1, average plaquette in column 2, fermion propagator at the origin (or $\langle \bar{\psi}\psi \rangle$) in column 3, dynamically generated fermion mass δm in column 4, and gauge-boson mass M in column 5.

β	$\langle 1 - \cos\theta_{\mu\nu} \rangle$	$\Delta(0)$	δm	M
0.00	1.00	0.246	0.47	∞
0.25	0.75	0.247	0.43	0.83
0.50	0.54	0.249	0.37	0.81
0.75	0.38	0.250	0.33	0.78
1.00	0.27	0.251	0.28	0.38
1.25	0.20	0.252	0.26	0.34
1.50	0.19	0.252	0.25	0.32
1.75	0.16	0.252	0.22	0.27
2.00	0.13	0.253	0.23	0.24
2.25	0.11	0.253	0.18	0.21
2.50	0.10	0.253	0.22	0.18
∞	0.00	0.254	0.00	0.00

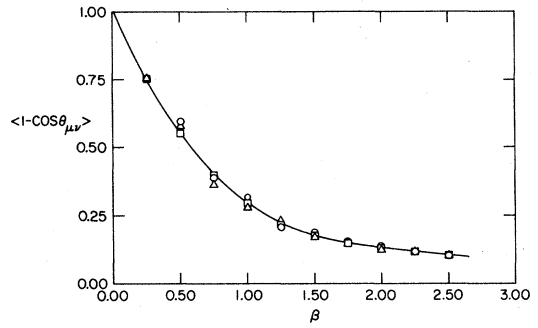

FIG. 2. The average plaquette $\langle 1-\cos\theta_{\mu\nu}\rangle$ as a function of β for $m=\infty$ (□), $m=0.5$ (△), and $m=0$ (○).

In the next figure (Fig. 3) we have plotted the inverse of $\langle\psi\psi\rangle$ versus the bare fermion mass squared (m^2). There is a marked tendency for this quantity to go to zero earlier (greater m^2) for larger β. Also the renormalized mass squared,

$$m_R^2=(m+\delta m)^2,$$

clearly appears to go to zero closer to $m^2=0$ for increasing values of β. We have estimated the critical mass squared to be $m_c^2=-2.0$, -1.5, -1.1, and -0.5 for $\beta=0.0$, 0.25, 0.5, and 1.0. From the location of the critical points at which

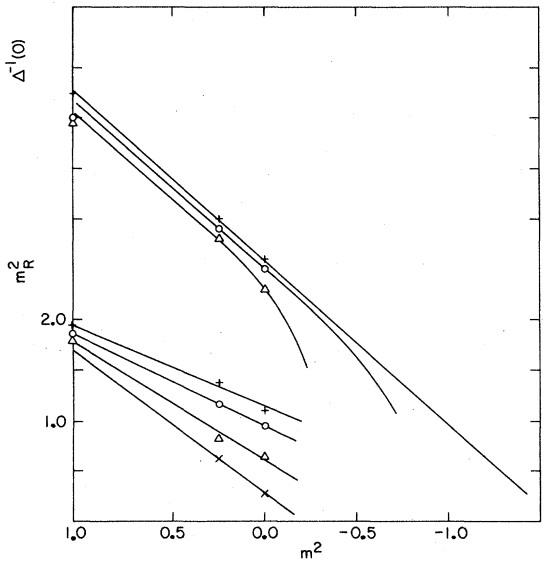

FIG. 3. The inverse of $\langle\bar{\psi}\psi\rangle$ (above) and the renormalized fermion mass squared (below) as a function of the bare mass squared. The points are for $\beta=0.25$ (+), $\beta=0.5$ (○), $\beta=1$ (△), and $\beta=1.5$ (×). The lines are drawn only as a guide to the eye.

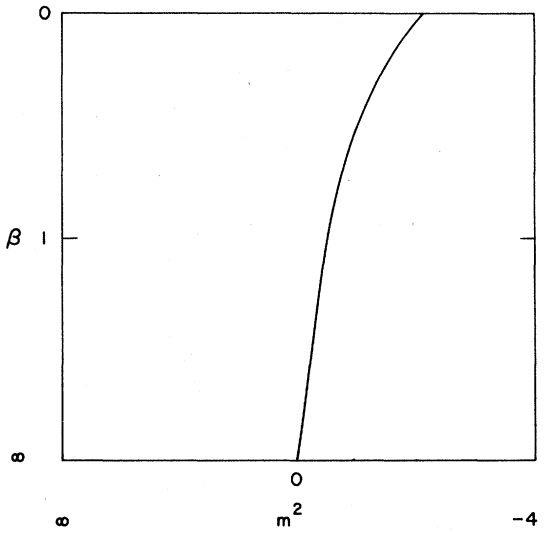

FIG. 4. The phase diagram of the theory in the $\beta-m^2$ plane. Along the curved line the renormalized mass vanishes.

$m_R^2=0$ at several values of β we have drawn the phase diagram shown in Fig. 4.

We mentioned that the Wilson loop has both area and perimeter behavior, one being more pronounced than the other depending (roughly) on the ratio β/k, at least for small β and k. As an illustration we show in Fig. 5 the β dependence of square loops $W(I)$ with sides of length I, where I varies from one to four, the largest meaningful size on a 10×10 lattice. The fermion mass m in this case was fixed at 0.5. One can see that the errors rapidly increase with the size of the loop. In Fig. 6 we have plotted the log of the square loop versus the length of its side. As β is decreased and k is increased (corresponding to a decrease in m) there is an indication of a change-

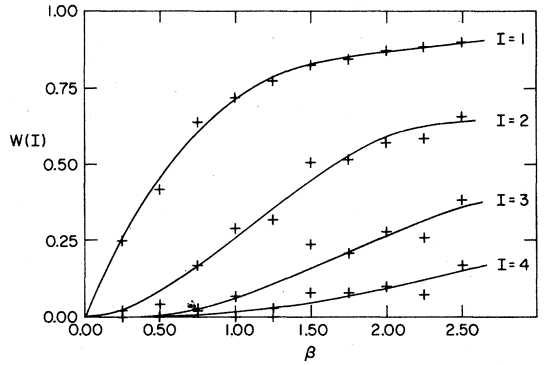

FIG. 5. Square Wilson loops $W(I)$ of sides I with $I=1$, 2, 3, and 4 as a function of β for $m=0.5$. The lines represent only a guide to the eye.

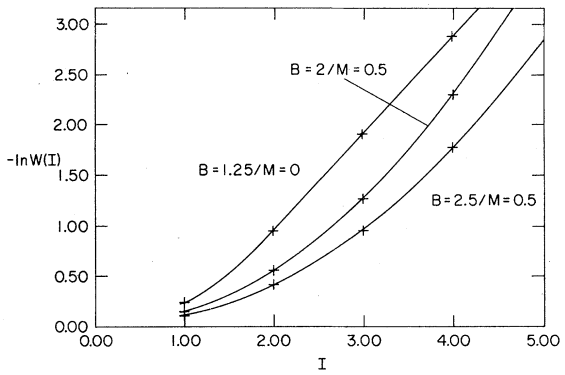

FIG. 6. Dependence of the logarithm of the square loop on the length of its side at fixed coupling. Data are for $m=0$, $\beta=1.25$ (○), $m=0.5$, $\beta=2.0$ (□), and $m=0.5$, $\beta=2.5$ (△). The perimeter behavior is clearly shown in the first case.

over from an area law to a perimeter law. A fit of the form $-\ln W(I)=AI^{\theta}$ gives $\theta\simeq 2.0$ in the case $m=0.5$, in agreement with an area dependence.

From the fermion and gauge-boson correlation functions we can extract their masses. The Monte Carlo runs were sufficiently long to determine the masses to an accuracy of the order of five percent. In the weak-coupling limit the renormalized fermion mass m_R approaches the bare mass m, whereas the boson mass and δm go to zero. For finite bare fermion mass one can easily convince oneself that for weak coupling

$$a^2\delta m^2=c_1g^2+O(g^3),$$
$$a^2M^2=c_2g^2+O(g^3),$$

where c_1 and c_2 are numerical constants, dependent on m, which can in principle be computed by evaluating numerically Feynman integrals with the appropriate lattice propagators and momenta limited to the first Brillouin zone. For $m=0$ we

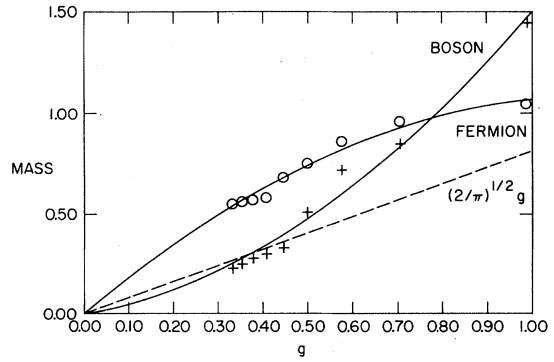

FIG. 7. Dynamic fermion mass δm (○) and boson mass M (+) as a function of $g=(1/4\beta)^{1/2}$ for $m=0$. The dashed line is $(2/\pi)^{1/2}g$.

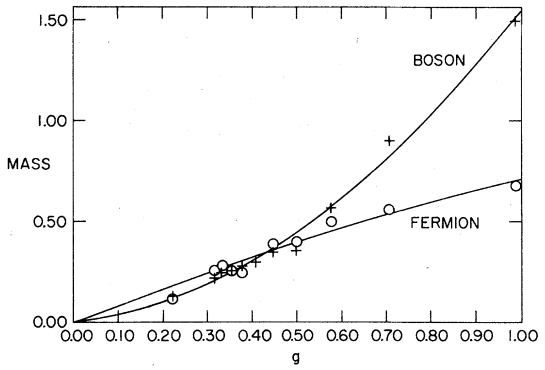

FIG. 8. Dynamic fermion mass δm (○) and boson mass M (+) as a function of $g=(1/4\beta)^{1/2}$ for $m=0.5$.

have shown before that

$$M=(2/\pi)^{1/2}g+O(g^2).$$

We have compared this prediction with our Monte Carlo data. For $m=0$ (see Fig. 7) M tends to follow the curve $(2/\pi)^{1/2}g$, consistent with the exact result for the Schwinger model. From our numerical data we would have estimated $M=(0.72\pm0.5)g[(2/\pi)^{1/2}=0.789]$. Of course, longer runs and larger lattices would allow a more precise determination of δm and M. For finite m both δm and M (see Fig. 8) approach zero. In Fig. 9 we have shown our results for the average $\langle\bar{\psi}\psi\rangle$.

In conclusion, we should mention that we have measured the connected meson-meson correlation function and found it to be consistent with zero to one part in 10^5 for most β and m.

V. CONCLUSIONS

We have shown how Monte Carlo simulations of systems with fermonic degrees of freedom can be used to compute correlations and mass gaps. With rather short runs on small lattices we have computed masses with an accuracy of the order of a few percent. We expect the results for the

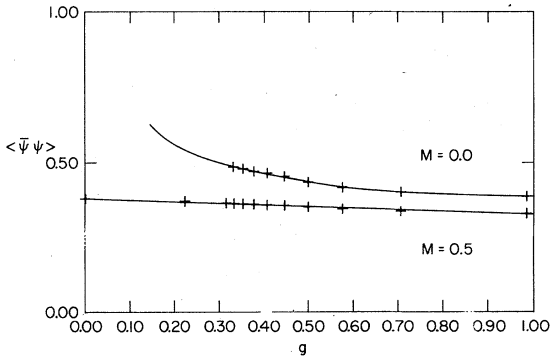

FIG. 9. The average $\langle\bar{\psi}\psi\rangle$ as a function of $g=(1/4\beta)^{1/2}$ for $m=0$ and $m=0.5$. The point at $g=0$ is exact.

phase diagram not to be qualitatively different for a confining theory in higher dimensions. The introduction of spin is also straightforward in this formulation. Although the method we have used is considerably slower (by a factor of $\sim 5 \times N^D$) than the usual Monte Carlo method, the convergence properties of the process are rather satisfactory. One might, therefore, expect quantitatively good answers by doing long runs at a few selected values of the parameters.

ACKNOWLEDGMENTS

The author wants to thank D. Scalapino, G. Bhanot, M. Creutz, V. Emery, and I. Muzinich for enlightening discussions. Thanks go also to the ISABELLE group for use of their VAX 11/780. This work was supported by the Division of Basic Energy Science, U. S. Department of Energy under Contract No. DE-AC02-76CH00016.

[1]F. Fucito, E. Marinari, G. Parisi, and C. Rebbi, CERN Report No. 2960, 1980 (unpublished).
[2]D. Scalapino and R. Sugar, Phys. Rev. Lett. 46, 519 (1981).
[3]D. Weingarten and D. Petcher, Phys. Lett. 99B, 333 (1981).
[4]L. D. Fadeev and V. N. Popov, Phys. Lett. 25B, 29 (1967).
[5]G. Parisi and N. Sourlas, LPTENS Report No. 80/8, 1980 (unpublished).
[6]J. Schwinger, Phys. Rev. 128, 2425 (1962).
[7]M. Bander, Phys. Rev. D 13, 1566 (1976).